ELSEVIER

Journal of Nuclear Materials 258–263 (1998) 1319–1323

journal of nuclear materials

Production of low activation steel; JLF-1, large heats – Current status and future plan [1]

A. Kohyama [a,*], Y. Kohno [b], M. Kuroda [a], A. Kimura [a], F. Wan [a]

[a] *Institute of Advanced Energy, Kyoto University, Gokasho, Uji, Kyoto 611, Japan*

[b] *Department of Materials Science, The University of Tokyo, Hongo, Bunkyo-ku, Tokyo 113, Japan*

Abstract

Based on the excellent basic properties prior to neutron irradiation and under neutron irradiation up to 100 dpa, the 9Cr–2W type low activation ferritic steel (LAF). JLF-1, had been selected as one of the reference materials to the IEA low activation ferritic steels R&D activity. This paper provides the general information about the second large heat of JLF-1 steel. The basic property of thick plates (24 and 12 mm in thickness) and their welded joints together with the information about microstructure are also provided.

1. Introduction

Many outstanding accomplishments in the areas of fusion science and plasma physics for several decades emphasize the urgent needs of R&D activities in the area of fusion engineering/technology. The consensus that "Materials are the Queen Technology of Fusion" or that "Materials are the Keys of fusion engineering/technology" has been widely recognized and many IEA activities on fusion materials have been initiated in recent years.

Presently, low activation ferritic steel (LAFs), vanadium alloys and SiC/SiC composite materials are considered promising candidates [1,2]. Among them, the R&D of LAFs is placed at the highest priority in the Japanese and the European programs [3,4].

To accelerate the development of LAFs, a working group under the Annex-II of the International Energy Agency (IEA) implementing agreement on a program of research and development on fusion materials has been formed to coordinate a collaborative program between the European Union (EU), USA and Japan. As one of the steels for the IEA test program, JLF-1 (a 9Cr–2W steel) steel has been provided from the Japanese university activity, JUPITER program. The first 1 metric ton heat of JLF-1 was produced in 1995 with a plate thickness of 7 and 15 mm. The second large heat of JLF-1 was produced in 1996. The 1.5 metric ton heat of JLF-1 steel was produced into plates with a thickness of 15 and 25 mm. The first large heat was mainly used to obtain basic mechanical properties and neutron and charged particle irradiation experiments including HFIR irradiation. The emphasis on the second large heat was to investigate joining technology and performance of the welded joints. Fracture toughness test using 25 mm thick plates is another important issue for the second heat.

The objective of this paper is to provide the recent information about the second large heat of JLF-1 steel and the future plan of R&D with irradiation studies. Although the chemical composition of the JLF-1 used for the IEA round-robin test is the same from the pre-IEA heats, the irradiation data of pre-IEA heat is provided elsewhere [5].

2. Production of the second heat

2.1. Fabrication procedure

An experimental alloy was melted in a 300 kg VIM furnace. The chemical composition is given in Refs [1,2].

* Corresponding author. Tel.: +81-774 38 3460; fax: +81-774 38 3467; e-mail: kohyama@iae.kyoto-u.ac.jp.

[1] Work supported by the Japan/USA Collaboration in Fusion Materials, "JUPITER Program".

0022-3115/98/$19.00 © 1998 Elsevier Science B.V. All rights reserved.
PII: S0022-3115(98)00198-6

The ingot was homogenized at 1250°C × 1 h, prior to forgoing into 100 mm thickness. The final rolling down 15 and 25 mm thickness was done at 1250°C × 3 h. The 15 and 25 mm thickness plates were sawed into $15 \times 330 \times 450$ and $25 \times 330 \times 500$ mm^3, respectively. Final heat treatments were normalized at 1050°C × 1 h/ air cooled (AC), followed by tempering at 780°C × 1 h/ AC. For the case of welded materials, post-welding heat treatment (PWHT) at 740°C × 3 h/AC was applied. The materials with normalizing and tempering were denoted as "as NT", and those with normalizing, tempering and PWHT were denoted as "NT + PWHT".

2.2. Basic mechanical properties

Tensile test results: As had been expected, the tensile properties were not dependent on the final plate thickness PWHT. The homogeneity in mechanical properties was excellent. Fig. 1 shows the tensile properties compared with F82H [6]. As shown in the figure, there were little differences in YS, UTS, Et and RA.

Creep rupture test results: Fig. 2 shows creep rupture strength compared with F82H [6]. Although the data on F82H were limited, the creep rupture properties were similar to those of JLF-1.

Charpy impact test results: Fig. 3 shows the results of JLF-1 together with the results of F82H [6], for comparison. The data of both JLF-1 and F82H were insufficient with a fair amount of scattering, to make a conclusive remark. The data on F82H were rolling direction dependent with a slight superiority for longitudinal direction over transverse direction. The data of JLF-1 looked independent of the rolling direction, but the data were insufficient and the rolling direction dependence is to some extent controllable with the production database in steel industries.

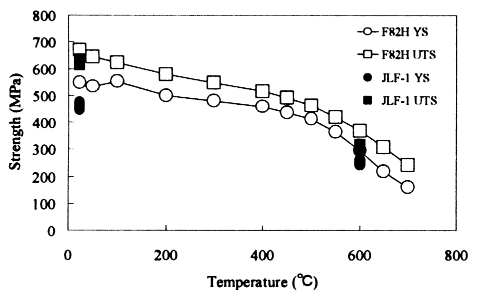

(a) 0.2% offset yield stress and ultimate tensile stress

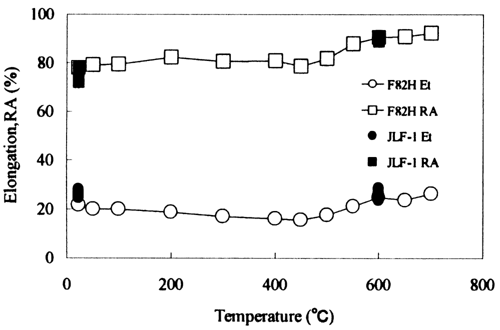

(b) Total elongation and reduction of area

Fig. 1. Tensile property compared with F82H stress.

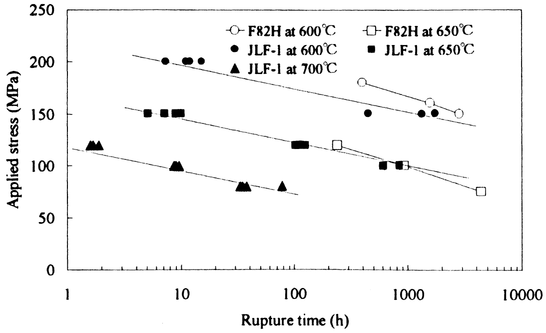

Fig. 2. Creep rupture strength compared with F82H.

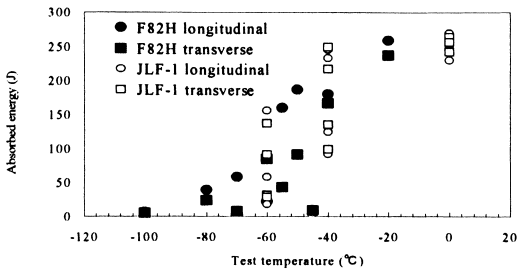

Fig. 3. Charpy impact properties compared with F82H.

3. Fabrication of welded joint

3.1. Fabrication procedure

Tungsten inert gas (TIG) welding was performed for the second heat. The chemical composition of welding wire and weld metal (WM) is given in Ref. [3]. TIG welding conditions are shown in Table 1. Also electron beam welding (EBW) was successfully done, and this is not given in this paper but is only given in Ref. [3].

3.2. Basic mechanical properties

Hardness distribution: Fig. 4 shows the macrostructure and hardness distribution of cross section of TIG-welded joints. The hardness of WM is about 20% higher than that of base metal (BM), and the lowest hardness

Table 1
TIG welding conditions

Plate thickness	15 mm, 25 mm
Current	230–250A
Voltage	10.5 V
Travel speed	10 cm/min
Heat input	14.5–15.8 KJ/cm
Pre heat temp	⩽ 200°C
Interlayer temp	⩽ 200°C
Number of passes	≠8, ≠20
Wire diameter	1.2 mm
PWHT condition	740°C × 3 h/F.C.

appears at the interface between BM and Heat Affected Zone (HAZ). To examine the difference of mechanical properties between BM and WM, some mechanical tests were conducted. The result was as follows.

Tensile properties: Tables 2 and 3 show the tensile properties of weld metal (WM) and welded joint (WJ). The position of fraction for WJ is always located in the area of BM. The reason why a fracture occurs in the area of BM in considered because of using a cylindrical type specimen, fracture ordinarily occurs at the position where the strength is relatively weak. This shows that WM has a higher strength in comparison with that of BM. Therefore the value of tensile properties of BM and WJ is almost the same. The change of tensile properties of WM is independent of the plate thickness.

Creep rupture test results: Compared with the values of BM and WM, time to rupture for WM is about 20% shorter than that of BM. The data compared with Larson–Miller parameter are shown in Fig. 5. According to the data, the value of both BM and WM 100 000 h 600°C rupture strength is about 100 MPa. It shows excellent properties as compared with other low-activation ferritic and austenitic steels:

as NT: $\sigma = -686\ln(\mathrm{P}) + 2205$,
NT + PWHT: $\sigma = -641(\mathrm{P}) + 2073$,
welded joint: $\sigma = -692\ln(\mathrm{P}) + 2218$.

According to F82H data [6], as follows:

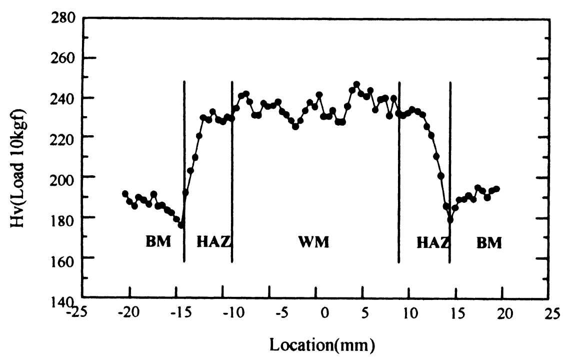

Fig. 4. Hardness distribution of TIG welds (plate thickness: 25 mm).

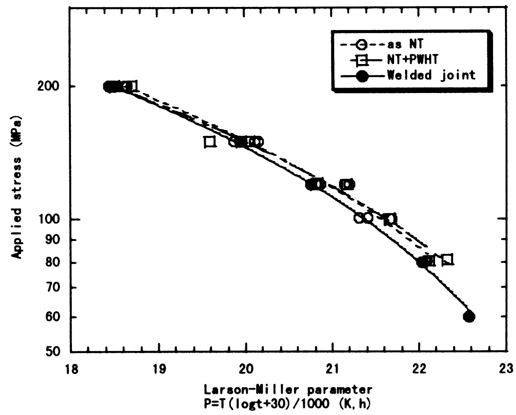

Fig. 5. Larson–Miller plot of JLF-1 steel and its weldment.

F82H: $\sigma = -1017\ \ln(P) + 3575$,
$P(K, h)$: $T(\log t + 30)/1000$.

Charpy impact test results: Table 4 shows the result of the charpy impact test. It is found that absorbed energy of WM is rather dependent on the plate thickness. It is ascertained that the value of absorbed energy of HAZ and WM is relatively lower than that of the other part. This means that HAZ and WM are brittle.

Fatigue test results: Fig. 6 shows the result of the fatigue test which was carried out under load controlled with hydraulic push–pull test machine. It was found that the fatigue life curve (*S–N* curve) cannot be given by a single linear line, and is bent with increase in applied stress amplitude. At increasing stress amplitude, it is considered that the influence of cyclic creep grows. So if the test is carried out under true stress controlled conditions and there is no influence of cyclic creep, it is expected that the fatigue life curve can be given by a single linear line.

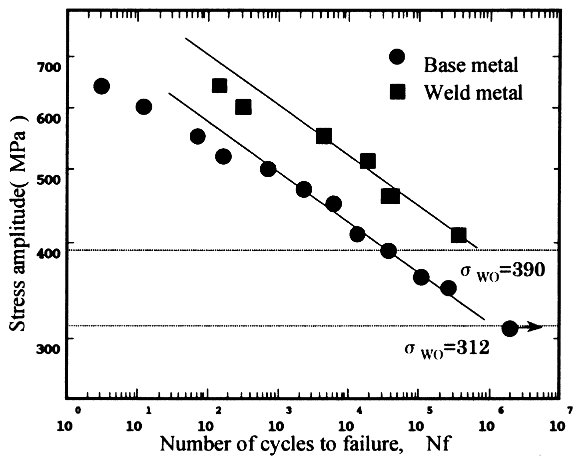

Fig. 6. Fatigue test result of JLF-1 steel and its weldment.

Table 2
Tensile properties of weld metal

Plate thickness (mm)	0.2% offset yield stress, YS (Mpa)	Ultimate tensile stress, UTS (Mpa)	Total elongation, (Et) (%)	Reduction of area, RA (%)
15	656	755	23.7	76.5
25	669	759	22.8	76.2

Heat treatment: PWHT.

Table 3
Tensile properties of weld joint

Plate thickness (mm)	Temperature (°C)	0.2% offset yield stress YS (Mpa)	Ultimate tensile stress UTS (MPa)	Total elongation Et (%)	Reduction of Area Ra (%)	Location of fracture
15	RT	447	610	18.9	74.8	BM
		448	611	20.1	79.7	BM
	600	250	293	19.3	89.4	BM
		256	294	20.3	89.8	BM
25	RT	464	619	21.7	77.3	BM
		466	619	19.6	75.1	BM
	600	256	308	20.2	88.3	BM
		260	307	21.0	87.9	BM

Heat treatment: PWHT.

Moreover, compared with the values of BM and WM, fatigue life for WM is considerably longer than that of BM. It is commonly well known that there is a good correlation between fatigue limit (σ_{wo}) and vickers hardness (H_V), σ_{wo} and tensile strength (σ_B):

$$\sigma_{wo} = 1.6H_V \times 0.1H_V \quad (H_V \leqslant 400),$$

$$\sigma_{wo} = 0.5\sigma_B.$$

Using this formula and Table 2, we can predict the values of fatigue limit of BM and WM. The values coincide well with the result of the fatigue test (see Fig. 6). Therefore we can explain why the fatigue life of WM is much longer.

3.3. Microstructure

According to an optical microscope observation, there is no great difference in the size and structure of grains of WM and BM. However, by an electron microscope some difference in microstructure can be observed. As shown in Fig. 7, many precipitates with a size of 100–200 nm formed along the grain boundaries of both WM and BM. On the other hand, there are a lot of small precipitates with a size of 10–30 nm in the grains of WM, but no such small precipitates can be observed in the grains of BM. The result of analyzing the electron diffraction patterns shows that the large precipitates are Cr23C6, and the small ones may be Cr7C3. It is

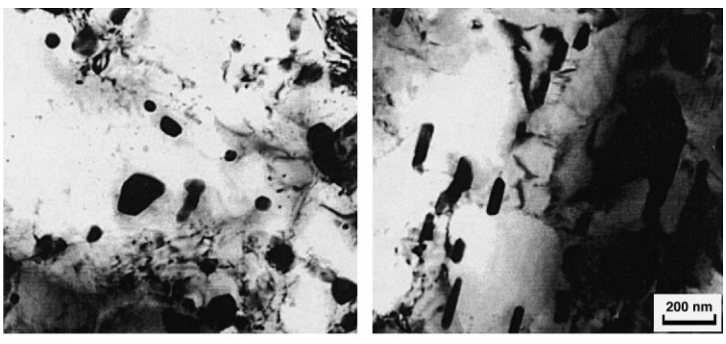

(a) Weld metal (a) Base metal

Fig. 7. Microstructure of base metal and weld metal by TEM.

Table 4
Charpy impact test result of JLF-1 steel

Plate thickness (nm)	Absorbed energy (J)				
	WM	FL	HAZ 1 mm	BM (longitudinal)	BM (transverse)
15	243	241	214	229	264
25	62	254	203	255	256

reasonable to consider that these small precipitates make WM harder and stronger than BM.

4. Future plan

The determination of basic mechanical properties as well as some physical properties are still ongoing and more extensive tests on fracture toughness, fatigue, creep, corrosion are to be conducted in the near future. Irradiation tests in HFIR, ATR, JOYO and JMTR are ongoing and in the planning stage. Also, ion irradiation, electron irradiation and multiple charged particle irradiation tests are ongoing. The preliminary study to see the effect of ferromagnetism is still in the planning stage in NIFS and IAE Kyoto University.

5. Conslusion

As an important part of the Japan/USA collaboration of Fusion Materials, JUPITER Program, the second large heat of JLF-1 was produced and the production of welded joints was successfully accomplished. The basic properties and some preliminary data on irradiation effects and microstructure stability obtained so far are quite promising for application to fusion reactors. The ongoing irradiation study in HFIR, JMTR and other future irradiation experiments are expected to provide more affirmative data that JLF-1 can be a candidate for the next fusion device, as well as for the fusion power reactor to be operated in the 21st century.

Acknowledgements

This work has been performed as one of the subtasks of the JUPITER Program, the authors would like to express their sincere appreciation to the members of the JUPITER Program for their support and encouragement. Special thanks are due Drs. T. Hasegawa and H. Mabuchi of Nippon Steel Corporation.

References

[1] Proceedings of International Conference on Fusion Reactor Materials, J. Nucl. Mater., Tokyo (1984), Chicago (1985), Kurlsrhue (1987), Kyoto (1989), Clearwater (1991), Stresa (1993), Obninsk (1995).
[2] A. Kohyama, H. Matsui, A. Hishinuma, Proceedings of 10th Pacific Basin Nuclear Conference, 1996, p. 883.
[3] Proceedings of the IEA Working Group Meeting on Ferritic/Martensitic Steels, Tokyo (1992), Oak Ridge (1993), Sun-Valley (1994), Oak Ridge (1995), Baden (1995), Culhum (1996).
[4] A. Kohyama, A. Hishinuma, D.S. Gelles, R.L. Klueh, W. Dietz, K. Ehrlich, J. Nucl. Mater. 233–237 (1996) 138.
[5] Y. Kohno, A. Kohyama, T. Hirose, M. Narui, presented at 8th Int. Conf. on Fusion Reactor Materials, Sendai, Japan, 1997.
[6] K. Shiba, A. Hishinuma, A. Tohyama, K. Masamura, JAERI-Tech 97–038.